NOTES

Comparison of Longwave Diurnal Models Applied to Simulations of the Earth Radiation Budget Experiment

DAVID R. BROOKS AND PATRICK MINNIS

Atmospheric Sciences Division, NASA Langley Research Center, Hampton, VA 23665

26 January 1983 and 11 October 1983

ABSTRACT

Simulations of the Earth Radiation Budget Experiment with several satellite sampling schemes have been used to compare three different approaches to modeling longwave diurnal behavior observed over certain kinds of land regions. November 1978 data from the GOES satellite have been used to produce a reference set of radiation parameters over the regions of interest. The monthly average longwave radiant exitance has been estimated first with linear interpolation between satellite measurements, then with a method that replaces linear interpolations across day–night boundaries with piecewise constant extrapolations to the boundaries, and finally with a trigonometric model which replaces some of the linear interpolations that go through daytime measurements over land. This third model consists of constant extrapolation of nighttime measurements to sunrise or sunset, with a half-sine curve fitted through existing daytime measurements and constrained at sunrise and sunset to an average of the surrounding nighttime measurements. It applies only when the daytime and surrounding nighttime measurements meet certain restrictive criteria, including tests that tend to limit the trigonometric model to cloud-free regions. For all satellite sampling strategies considered, the trigonometric model gave the best overall monthly estimate of longwave radiant exitance. For non-land regions, the linear interpolation model generally gave better results than the piecewise constant model.

1. Introduction

The Earth Radiation Budget Experiment (ERBE) is a multi-satellite experiment planned for implementation in the mid 1980's (Woerner *et al.*, 1978). It will consist of instruments on one or more Sun-synchronous satellites in the NOAA series, and a dedicated spacecraft, the ERBS, in a 57° orbit. One of the primary objectives of the ERBE is to improve knowledge of diurnal variability in the Earth's radiation balance. The primary diurnal effect is the Sun-driven variability in reflected (shortwave) radiation. However, many land areas of the Earth also exhibit regular diurnal variations in emitted (longwave) radiation due to surface temperature fluctuations. Such longwave (LW) behavior can easily be seen over cloud-free land, and it is especially prominent over desert areas where the day–night variation of LW radiation can be on the order of 100 W m^{-2}. Regular diurnal cycles in cloudiness can produce observable LW cycles over some ocean regions, but these are substantially smaller than the cycles typically observed over land. Modeling of LW diurnal cycles is important to the ERBE project because the analysis procedures specifically preclude the use of auxiliary data (as from geostationary satellites) for routine processing of flight data.

In previous analyses of satellite radiation data, the monthly average longwave flux has been obtained by averaging daytime and nighttime measurements. For Nimbus 2 and 3, the day–night pairs of narrow-field-of-view measurements were weighted according to the length of day and night (Raschke and Bandeen, 1970; Raschke *et al.*,1973). For some other analyses, including those using data from non-Sun-synchronous satellites, simple averages of LW data appear to have been used (Bandeen *et al.*, 1965; Gruber and Winston, 1978; Jacobowitz *et al.*, 1979). For this note, satellite samples of LW radiation over land are simulated for both Sun-synchronous and non-Sun-synchronous orbits. Three different LW diurnal models are then applied to the sampled data, and the resulting modeled monthly net LW radiant exitances are compared against reference values based on complete hourly sampling of the area for a month. Such comparisons will be used to define processing algorithms for the ERBE satellite system. In addition, they could be used to understand possible biases in previous satellite data, and also to better define those areas in which LW diurnal variability plays a substantial role in the radiation balance.

2. Data base and sampling strategy

This study utilizes a detailed analysis (Minnis and Harrison, 1984a) of November 1978 data from one of the Geostationary Operational Environmental Satellites (GOES-east, hereinafter referred to as GOES). The coverage area extends from 45°N to 45°S and is centered over North and South America at about 75°W. The area is divided into 1600 regions ranging

from 2.25° × 2.25° at the Equator (about 250 km × 250 km) to 2.25° × 3° at ±45° latitude. These regions are considered to be sufficiently close to the 2.5° × 2.5° ERBE grid system (Brooks, 1981) to allow application of simulation studies to analysis of the ERBE mission itself.

Satellite sampling of the GOES regions is driven by orbit propagation programs that predict temporal coverage for each region. Representative monthly LW samples simulated for an early afternoon Sun-synchronous orbit and the ERBS at 57° are shown in Table 1. A 2:30 p.m. orbit is considered the most likely situation for the ERBE. The 30 × 24 matrix represents each day and local hour for the month of November. An hour index of 1 represents the local times between 12:00 a.m. and 1:00 a.m. The regional reference data from GOES include a LW radiant exitance in each of the 720 day–hour locations. Sun-synchronous orbits restrict the coverage so that only a few local hours are sampled during the month. The ERBS samples, on the other hand, precess through 24 h of local time in about 73 days. Because LW measurements are made during both day and night, all local hours are filled in after about 36 days. In both cases the spread of samples across a few hours is due to the operating mode assumed for a scanning narrow-field-of-view radiometer which will be one of the ERBE instruments.

TABLE 1. Representative longwave satellite sampling patterns for Sun-synchronous and non-Sun-synchronous orbits (in GOES region 1145).

	1430 LST SS orbit			57° ERBS orbit		
	Local hour index					
Day	1	13	24	1	13	24
1	x	x		x x		x
2	x	x		x		xx
3	x	x		x x		x
4	x	x		x x		x
5	x	x		x		xx
6	x	x		x x		x
7	x x	x		x x		x
8	x x	x		xx		xx
9	x x	xx		x		x
10	x x	xx		x x		x
11	x x	xx		x		xx
12	x x	xx		x x		x
13	xx	x x		x x		x
14	xx	x x		x		x
15	x	x x		x x		x
16	x	x x		x		x
17	x	x		xx		x
18	x	x		x x		xx
19	x	x		x		x
20	x	x		x		x
21	x	x		x x		xx
22	x	x		x		x
23	x	x		x		x
24	x	x		x x		xx
25	x x	x		x		x x
26	x x	x		x		x
27	x x	x		x x		xx
28	x x	xx		x		x x
29	x x	xx		x		x x
30	x x	xx		x		xx

3. Application of longwave models to satellite samples

Reference values of longwave radiant exitance (LWRE) are shown as the circular symbols in Fig. 1 for 17–19 November 1978, in a South American region that includes parts of the Atacama Desert and the Salar de Uyuni salt flats. This is not intended to be typical of land regions, but it falls within the category of land regions exhibiting high LW variability and is used here to accentuate the differences between the models used. Each reference LWRE is assumed to correspond to the half hour at each local hour. The locations of satellite samples from the simulated Sun-synchronous orbit are indicated by filled symbols. Three different models have been applied to these data, each of which produces LWRE values corresponding to the local half hour in each empty hour box. The first model uses linear interpolation to fill in the missing hours. The results of applying this model are identified by the solid line in Fig. 1. The linear interpolation model ignores specific diurnal variations in favor of filling in the entire month with a piecewise linear curve. The first and last available measurements on Fig. 1 are extrapolated backward or forward to measurements on days 16 and 20, respectively.

The second model responds to diurnal effects by using piecewise constant extrapolations to day–night boundaries. To do this, each hour box is given a day or night designation for the region and time of year. Linear interpolations that cross day–night boundaries are replaced by constant extrapolations to the boundary from both sides. This piecewise constant model is similar to weighting day and night measurements by the length of day and night at the time and place of the measurements. The results are indicated by the broken line in Fig. 1. For the sampling illustrated here, there are no remaining linear interpolations because there is only one measurement for each day and night period.

The third model is based on the observation by Minnis and Harrison (1984b) that many cloud-free land regions in the GOES field of view exhibit a repeatable LW diurnal pattern consisting of fairly uniform nighttime temperatures with warmer daytime temperatures that peak near local solar noon. Similar patterns have been observed in METEOSAT data (Saunders and Hunt, 1980); they contrast sharply with typical LW diurnal behavior for cloudy and non-land surfaces. This observed daytime behavior can be approximated by a half-sine-shaped curve. To implement this model, the linear interpolation model is first applied to the entire month. Data taken over land regions are then searched for points that straddle day–night boundaries. If there are one or more daylight points surrounded by nighttime data on both sides, then the model may be applied. If any of the daytime points are less than or equal to either nighttime point (as would typically happen over cloudy land), then it is assumed that the predicted diurnal behavior will not

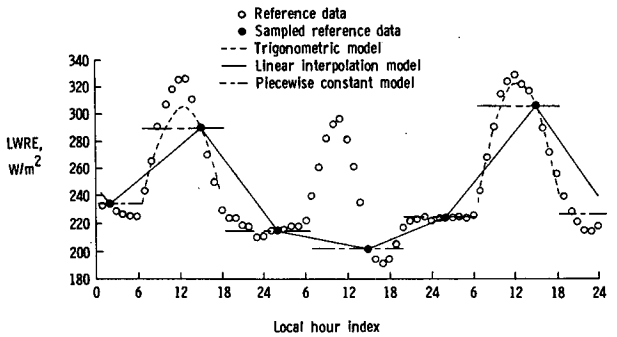

FIG. 1. Application of longwave models to 17–19 November 1978 over a GOES land region in South America, for a simulated 1430 LST Sun-synchronous orbit.

occur and the linear interpolation model is retained. If the model appears to be applicable to the observed data, a half-sine curve is calculated to fill in all the daylight hours. It is constrained to be equal to the average of the surrounding nighttime points at the day–night boundaries, and is fit to the available daytime points with a standard least squares technique. Specifically, the LW model for daytime is then of the form

$$y(t) = \mathrm{LWRE}(t) - \overline{\mathrm{LWRE}}(\mathrm{night}) = a \sin(90°t/h), \quad (1)$$

where a is a constant to be determined from the daytime data, t the time in hours from sunrise, $\overline{\mathrm{LWRE}}$ $\times$ (night) is the average of the preceding and following nighttime values, and h is the half-day length in hours. For a set of N daytime measurements, the least squares value of a is given by

$$a = \frac{\sum_{i=1}^{N} y_i \sin(90°t_i/h)}{\sum_{i=1}^{N} \sin^2(90°t_i/h)}. \quad (2)$$

The model is applied at the local half hour. It is not applied at all in those cases where daytime points lie only in the first and/or last daylight hour. This prevents the generation of unreasonably large midday peaks from an insufficiently constrained situation. The results of applying this trigonometric model are indicated by the dashed line in Fig. 1. The criteria for applying the trigonometric model have been met on days 17 and 19, but not on day 18, where a cold (assumed to be cloudy) early afternoon scene was measured. Note that none of the models has successfully retrieved the LW behavior of the second day. This is due to sparse measurements on a day with highly variable cloud cover.

Each of the LW models has been applied to two different sets of 40 GOES land regions for the entire month of November 1978. For each region, the reference LWRE at each hour has been averaged over the month. The daily range of the monthly hourly average (mha) is then defined as the difference between the maximum and minimum mha. One set of 40 regions was chosen to represent areas with high mha daily ranges. Of these, 20 are near the western coast of South America south of about 20°S, 18 are in the American Rockies and southwest, and 2 lower-variability comparison regions are located south of the Great Lakes. The region from which the data for Fig. 1 were taken is representative of the high-variability regions, with an mha range of 79 W m^{-2}. In the second set, 40 regions were randomly selected from the remaining available land areas. (One of the regions is common to both sets, for internal checks.) The location of both sets of land regions, as well as a set of 30 ocean regions, are given in Fig. 2.

The two-orbit sampling schemes previously described have been used to simulate the retrieval of LW diurnal behavior with each of the three LW models. The results are summarized in Table 2, which gives for each case the maximum, minimum and mean bias μ (where bias is defined as reference minus model value) and sample standard deviation s. The last two values are combined to produce the standard error of estimate ϵ, where $\epsilon^2 = s^2 + \mu^2$. The Sun-synchronous results may be compared with those from ERBS sampling over the same 40 high-variability regions. In both case ϵ is smallest for the trigonometric model, while the relative performance of the piecewise constant and linear interpolation models depends on the sampling method.

It is expected that the comparative performance of the LW models will depend on the choice of regions.

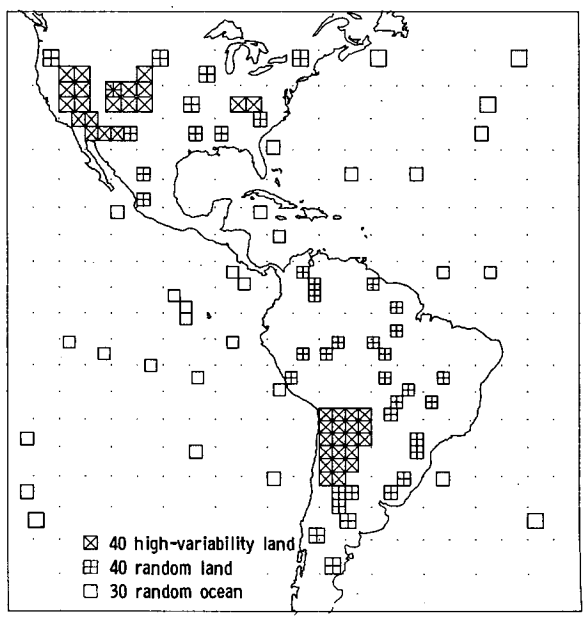

FIG. 2. Distribution of regions for longwave diurnal modeling simulations.

TABLE 2. Summary of simulated retrieval of monthly average longwave radiant exitance over various land and ocean regions, using two different satellite orbits and three LW diurnal models.

Regions	Sample type	Parameter	LWRE bias ($W m^{-2}$) for model type:* LI	PC	TR	Average TR days†
40 high-variability land (average mha range = 44.6 Wm^{-2})	PM SS	maximum bias	−0.9	−0.3	3.8	21.4
		minimum bias	−6.1	−10.8	−4.3	
		μ	−3.4	−4.2	0.8	
		s	1.3	2.9	1.6	
		ϵ	3.6	5.1	1.8	
	ERBS	maximum bias	11.6	6.9	6.6	14.1
		minimum bias	−6.1	−4.8	−2.9	
		μ	1.0	3.7	0.5	
		s	5.5	1.0	2.8	
		ϵ	5.6	3.9	2.8	
40 random land (average mha range = 28.9 W m^{-2})	PM SS	maximum bias	1.5	1.1	4.6	16.5
		minimum bias	−6.0	−6.4	−3.6	
		μ	−2.0	−2.3	0.5	
		s	1.8	2.2	1.8	
		ϵ	2.7	3.1	1.9	
	ERBS	maximum bias	7.9	6.3	4.1	10.5
		minimum bias	−3.9	−4.8	−4.9	
		μ	1.3	0.7	0.6	
		s	3.5	2.9	2.2	
		ϵ	3.7	3.0	2.3	
30 ocean (average mha range = 8.9 W m^{-2})	PM SS	maximum bias	2.0	2.0		
		minimum bias	−2.0	−2.0		
		μ	−0.1	−0.2		
		s	0.9	0.9		
		ϵ	0.9	0.9		
	ERBS	maximum bias	3.9	2.3		
		minimum bias	−2.3	−2.5		
		μ	0.3	0.4		
		s	1.2	1.0		
		ϵ	1.2	1.1		
40 high-variability land	PM SS + ERBS	maximum bias	0.7	0.3	2.9	16.2
		minimum bias	−3.4	−6.2	−1.7	
		μ	−1.1	−2.3	0.2	
		s	1.1	1.7	1.1	
		ϵ	1.6	2.8	1.1	

* LI, linear interpolation; PC, piecewise constant; TR, trigonometric.
† Average numbers of days on which trigonometric model was applied.

A second set of regions has been selected at random from the remaining GOES land regions; they are characterized by a lower average mha LW diurnal range (28.9 versus 44.6 W m^{-2}) and fewer days on the average in which the trigonometric model can be applied (10.5 versus 14.1 days for the ERBS orbit and 16.5 versus 21.4 days for the Sun-synchronous orbit). The results of LW modeling over these regions are summarized in Table 2. Again, for each type of sampling, the trigonometric model is superior to the other two.

By definition, the trigonometric model applies only over land. To compare the linear interpolation and piecewise constant models over water, 30 random ocean regions have been examined. These ocean regions, dominated by the western Pacific Ocean, have an average mha LW range of only 8.9 W m^{-2}. The linear interpolation and piecewise constant models both perform better over ocean than over land for the sampling assumed. As with the other sets of regions, the relative performance of the models is a function of sampling.

When multiple satellite sampling is available, all the time and space averaging models for diurnal behavior are expected to perform better because more mea-

surements are available throughout the day. To illustrate the expected improvement in average LW estimates, the ERBS and Sun-synchronous samples have been combined over the high variability land regions. The results of LW modeling from these samples are given as the final entries in Table 2; the three LW models give average monthly biases of −1.1, −2.3 and 0.2 W m^{-2}, respectively. This is a substantial improvement over single-satellite sampling in each case, and the trigonometric model shows the most improvement.

The influence of orbit plane orientation (equivalent to local time) on the ability of single satellites to retrieve monthly average LWRE at any hour is evident in the standard errors of estimate for mha LWRE shown for the 24 local hour indices in Figs. 3a and b. These data are given for Sun-synchronous and ERBS sampling over the 40 high-variability land regions. All the models suffer in daylight hours near the day-night boundaries when only Sun-synchronous data are available. This is because the relatively high temperatures recorded in the early afternoon do not apply to the rest of the daytime hours, especially for the piecewise constant model. If diurnal averages based just on measurements at a single hour are used without a model, pronounced biases are to be expected in these highly variable regions. Such biases have been noted in desert regions by Saunders and Hunt (1980) when they compared the LW diurnal mean from hourly METEOSAT data over the western Sahara Desert to a single value at 9 a.m. local time. In that case, the morning measurement was about 3% higher than the actual diurnal mean, a value that is consistent with comparable observations of the GOES data set. It is expected that for near-noon Sun-synchronous orbits like those of the Nimbus series, diurnal averages based on linear interpolation or piecewise constant models will produce errors over land that are consistently larger than those based on the trigonometric model.[1]

For the ERBS case studied here, the presence of some data throughout the entire day helps to improve mha LWRE near the day–night boundaries, but at the expense of underestimating midday temperatures. Any given orbit plane orientation will favor some hours over others, but the variable local measurement time during a month prevents any single hour from being estimated as accurately as the Sun-synchronous sample at its nearly constant local measurement time. As expected, the trigonometric model is very close to the piecewise constant model at night because it also utilizes a piecewise constant extrapolation to the day–night boundary. The better performance of the trigonometric model under all conditions indicates that both the assumed half-sine shape and the applied constraints are reasonable.

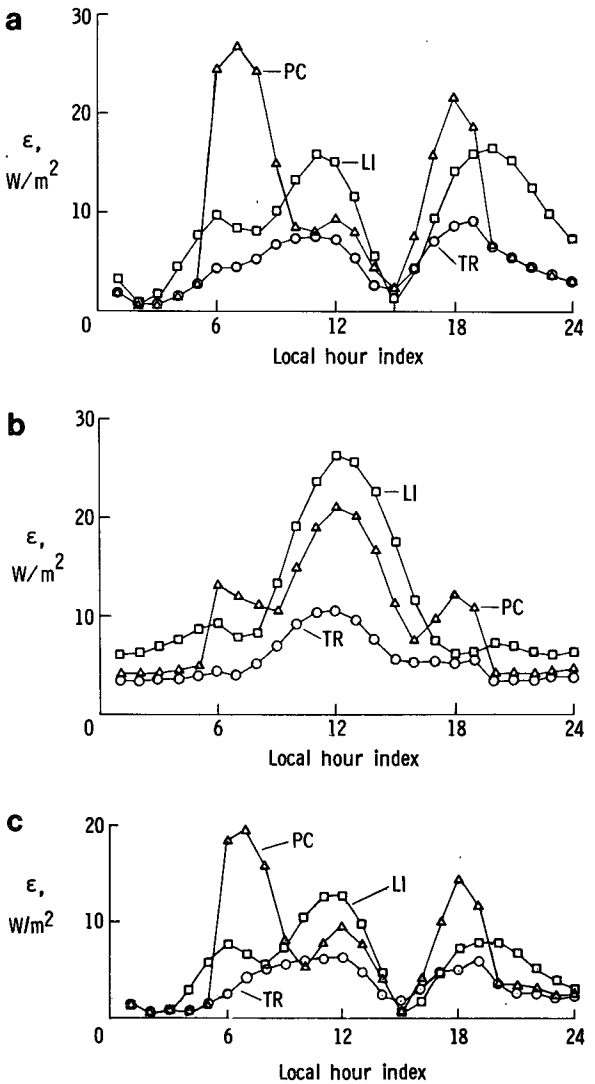

FIG. 3. Standard error of estimate for monthly hourly longwave radiant exitance, for three longwave models and three simulated sampling strategies, applied to 40 high-variability GOES land regions in November 1978: (a) 1430 LST Sun-synchronous; (b) 57° ERBS orbit; (c) ERBS plus 1430 LST Sun-synchronous orbit.

Monthly hourly average estimates of LWRE obtained from the two-satellite sample (ERBS and Sun-synchronous) are shown in Fig. 3c. While all the models give better daily average LWRE estimates with two satellites than with one, the behavior of the piecewise constant model at individual hours is quite erratic. For example, the addition of ERBS samples to the Sun-synchronous sample does little to improve the piecewise constant model at the day–night boundaries. To put it another way, addition of Sun-synchronous samples to ERBS samples may actually deteriorate the ERBS estimate of mha LWRE for early-morning or

[1] See Appendix L of Minutes of a Special ERBE Inversion Workshop to Assess Scene Identification and Angular Modeling Techniques, 16–17 Feb. 1982, ERBE Document 3-3-5-S2-82-02-00, NASA Langley Research Center, Hampton, VA.

late-afternoon hours when constant extrapolations are made to the day–night boundary.

It is interesting to note that the average number of days for which the trigonometric model applies to the two-satellite case (16.2 days) is only slightly above the value for the single ERBS orbit (14.1 days), rather than near or higher than the Sun-synchronous value (21.4 days). This is because the additional sampling reveals the presence of clouds (lower daytime temperatures) that are overlooked with fewer samples, and these data prevent the inappropriate application of the trigonometric model.

4. Conclusions

The general usefulness of a trigonometric diurnal LW model for land regions with daytime heating trends has been demonstrated by simulations over substantial portions of the land areas within the GOES field of view. While these results are observed to be scene- and orbit-dependent, the largest regional biases in retrieved monthly average LWRE, on the order of ± 10 W m^{-2}, have consistently been obtained when the linear interpolation or piecewise constant models are applied to satellite samples. The sign of these regional biases depends on the interrelationship between the sampling model and the temporal distribution of measurements. Application of the trigonometric model under appropriate circumstances reduces both the standard deviation and the range of bias error within any given set of land regions. For a set of 40 regions with high LW variability, the standard error of estimate of monthly average LWRE has been significantly reduced from about 4–6 W m^{-2} to about 2–3 W m^{-2} for the regions and sampling strategies studied. Note that the errors will be lower than this over most of the globe, where LW diurnal variability is not as significant.

The linear interpolation model has been shown to be a reasonable choice for nonland regions, and it applies equally well to land regions with measurements that are poorly timed or that indicate the presence of cloud cover so that the trigonometric model should not be used. There is no apparent reason to choose the piecewise constant model for data processing on the Earth Radiation Budget Experiment since it often produces larger biases than the linear interpolation model and requires more computation time as well.

In contrast to shortwave diurnal modeling, which is specifically scene-dependent, these LW models do not require scene identification information. Hence they could be applied retroactively to previous satellite data. Knowledge of the satellite ground track history is the only additional requirement for the appropriate application of the TR model to land areas.

Acknowledgments. We would like to thank Mr. Gary G. Gibson, Kentron International, Hampton Technical Center, Hampton, Virginia for his preparation of the orbit-driven data sampling tapes used in this study.

REFERENCES

Bandeen, W. R., M. Halev and I. Strange, 1965: A radiation climatology in the visible and infrared from the Tiros Meteorological Satellites. NASA TN D-2534, 30 pp. [NTIS N65-24522].

Brooks, D. R.,, 1981: Grid systems for Earth Radiation Budget Experiment applications. NASA TM-83233, 39 pp. [NTIS N82-14818].

Gruber, A., and J. S. Winston, 1978: Earth–atmosphere radiative heating based on NOAA scanning radiometer measurements. *Bull. Amer. Meteor Soc.*, **59**, 1570–1573.

Jacobowitz, H., W. L. Smith, H. B. Howell, F. W. Nagle and J. A. Hickey, 1979: The first 18 months of planetary radiation budget measurements from the Nimbus-6 ERB experiment. *J. Atmos. Sci.*, **36**, 501–507.

Minnis, P., and E. F. Harrison, 1984a: Diurnal variability of regional cloud and surface radiative parameters derived from GOES data. Part III: November 1978 radiative parameters. Submitted to *J. Climate Appl. Meteor.*

——, and ——, 1984b: Diurnal variability of regional cloud and surface radiative parameters derived from GOES data. Part I: Analysis method. Submitted to *J. Climate Appl. Meteor.*

Raschke, E., and W. R. Bandeen, 1970: The radiation balance of the planet Earth from radiation measurements of the satellite Nimbus II. *J. Appl. Meteor.*, **9**, 215–238.

——, T. H. Vonder Haar, M. Pasternak and W. R. Bandeen, 1973: The radiation balance of the Earth atmosphere system from Nimbus 3 radiation measurements. NASA TN D-7249, 76 pp. [NTIS N73-21702].

Saunders, R. W., and G. E. Hunt, 1980: METEOSAT observations of diurnal variation of radiation budget parameters. *Nature*, **283**, 645–647.

Woerner, C. V., J. E. Cooper and E. F. Harrison, 1978: The Earth radiation budget satellite system for climate research. COSPAR, Advances in Space Exploration, **4**, *Remote Sounding of the Atmosphere from Space*, H. J. Bolle, Ed., 201–215.